МРНТИ 31.15.23

https://doi.org/10.18321/cpc23(3)371-381

Electrochemical Recovery of Iron from Sulfuric Acid Leachates of Coal Ash

A. Batkal*, K. Kamunur, M.T. Yskak, L.K. Beisembaeva

¹Al-Farabi Kazakh National University, al-Farabi ave., 71, Almaty, Kazakhstan

ARTICLE INFO

Received 09.08.2025

Received in revised form 19.09.2025

Accepted 06.10.2025

Keywords:

coal ash; sulfuric acid leaching; electrodeposition; electrochemical iron recovery; resource utilization

ABSTRACT

Coal ash represents a major industrial by-product containing significant amounts of iron, yet its recovery is hindered by the inert aluminosilicate matrix. In this study, a two-step approach was developed for selective extraction and electrochemical recovery of iron. Coal ash was first treated with concentrated sulfuric acid at elevated temperature, producing a leachate enriched in Fe²⁺ ions. The effects of Fe²⁺ concentration (0.1-0.5 mol/L), current density (1250-5000 A/m²), and electrolysis time (1-6 h) on recovery efficiency, current efficiency, and energy consumption were systematically investigated. Under optimal conditions (0.30 mol/L Fe²⁺, 2500 A/m², 4 h), iron recovery reached 89% with a current efficiency of 65%, while energy consumption was as low as 1.8 Wh/L. XRD and SEM analyses confirmed that optimized parameters favor the formation of metallic Fe with minor magnetite content. These results demonstrate the feasibility of integrating acid leaching and electrolysis into a practical route for coal ash valorization and selective iron recovery.

1. Introduction

Coal combustion by-product, particularly coal ash, represent one of the largest industrial solid wastes worldwide. Their continuous accumulation poses serious environmental and disposal challenges due to the vast volumes generated and the presence of hazardous constituents. At the same time, coal ash is recognized as a valuable secondary resource because of its substantial content of oxides such as SiO_2 , Al_2O_3 , and Fe_2O_3 , along with minor but technologically important trace elements [1-4]. Utilizing this waste stream as a resource not only reduces the burden of disposal but also contributes to the sustainable supply of raw materials.

Various strategies have been explored for the utilization of coal ash, including mechanical separation, pyrometallurgical processing, and hydrometallurgical treatments. Mechanical beneficiation can partially concentrate ferromagnetic phases but typically suffers from low selectivity [5,6]. Pyrometallurgical methods allow iron recovery in the form of pig iron or alloys but are energy-intensive and require high operating temperatures [7]. Hydrometallurgical approaches, particularly acid leaching, are effective in dissolving iron together with other matrix components, but the subsequent separation and purification steps remain challenging [8-10].

Iron is typically one of the major components of coal fly ash, present mainly as hematite (Fe_2O_3), magnetite (Fe_3O_4), and aluminosilicate-bound forms [11-13]. With concentrations often exceeding 15 wt%, iron represents the most abundant recoverable metal in ash. Its selective extraction is of interest not only for resource recovery but also for improving the performance of ash in secondary applications, such as construction materials.

Acid leaching is widely applied to obtain leachates from coal ash [14-18]. Among different mineral acids, sulfuric acid is often preferred due to its strong solubilization power, availability, and relatively low cost [19-22]. The acidic environment minimizes hydrolysis of ferric iron and suppresses the premature precipitation of hydroxides, thereby producing stable leachates suitable for further processing.

Electrolysis offers an attractive route for recovering iron directly from aqueous leachates [23-25]. In comparison to chemical precipitation or solvent extraction, the electrochemical approach enables controlled deposition of metallic iron with high selectivity and reduced chemical reagent consumption. Electrochemical treatment has the advantage of producing value-added metallic iron while simultaneously reducing waste generation. Despite these benefits, the systematic study of

Corresponding author: A. Batkal *E-mail address: abatkalova@mail.ru

electrolytic iron recovery from coal ash leachates remains limited, highlighting the need for further investigation.

Despite numerous studies on coal ash utilization [26], systematic investigations of electrochemical iron recovery from leachates remain scarce. In particular, the combined influence of Fe²⁺ concentration, current density, and electrolysis duration on recovery efficiency, energy demand, deposit characteristics has not been comprehensively addressed. To fill this gap, the present work develops and evaluates a two-step process consisting of concentrated sulfuric acid leaching of coal ash to obtain Fe2+ -rich solutions and subsequent electrochemical recovery of iron under controlled operational conditions. The effects of key parameters are systematically assessed, and the resulting deposits are characterized to elucidate their phase composition and morphology. By establishing optimal electrolysis conditions and benchmarking the outcomes against recent literature, this study provides new insights into the feasibility and potential scalability of electrochemical iron recovery from coal ash leachates.

2. Materials and Methods

2.1. Raw material and characterization

The coal ash (CA) used in this study was obtained from a coal-fired thermal power station – 2 (Almaty) and exhibited the following oxide composition (wt%): $SiO_2 - 52.67$, $Al_2O_3 - 21.39$, $Fe_2O_3 - 17.24$, CaO - 6.23, and MgO - 2.05. The CA was dried at 105 °C and ground to pass through a 75 μ m sieve prior to use.

2.2. Acid leaching procedure

To extract iron from CA, 100 g of the ash was mixed with 500 mL of concentrated sulfuric acid (95-98 wt%). The mixture was baked at 200 °C for 4 h. Upon cooling to room temperature, the resulting clinker was leached with 500 mL of distilled water under constant stirring at 95 °C for 1 h. The leachate was separated from the residue via vacuum filtration (Büchner funnel).

2.3. Electrolysis setup and procedure

Electrochemical experiments were carried out in a 1 L cylindrical glass cell at ambient temperature (25 \pm 2 °C). A titanium plates (7 cm²) served as both

the anode and as the cathode. The interelectrode distance was fixed at 2 cm. The electrolyte was the leachate obtained above, supplemented where necessary with $FeSO_4 \cdot 7H_2O$ to achieve desired Fe^{2+} concentrations (0.1-0.5 M). The electrodes were connected to a QJ1503C DC power supply (QJE, China), operated under galvanostatic mode. The influence of three main parameters was investigated: Fe^{2+} concentration (0.1-0.5 M), current density (1250-5000 A/m²), electrolysis time (1-6 h).

After electrolysis, the solid precipitate was collected, washed thoroughly with distilled water, and dried at 60 $^{\circ}\text{C}$ for characterization.

2.4. Analytical methods

The elemental composition of solid samples was determined by X-ray fluorescence spectrometry by using XRF spectrometer (Malvern Panalytical, UK / Netherlands).

Elemental concentrations in leachates were determined using atomic absorption spectroscopy (GBC Savant, Australia). The concentration of ferrous iron (Fe²+) was measured spectrophotometrically using 1,10-phenanthroline on a CΦ-2000 (Russia) at λ = 510 nm. Ferric iron (Fe³+) was estimated by difference after total iron determination. The crystalline phases of the precipitates were identified by DW-27 Mini diffractometer (DFMC, Dandong, China) with Cu K α radiation. Bulk pH of the solution during electrolysis was monitored with a calibrated pH meter ITAN-G pH-meter/ionometer (Russia). Scanning electron microscopy (SEM) was performed by using a Quanta 200i 3D microscope (FEI Company, USA).

3. Results and Discussion

3.1. Feasibility study

Table 1 presents the oxide composition of the coal fly ash used in this study, as determined by X-ray fluorescence (XRF).

Table 1. Composition of initial coal ash (wt%)

Component	SiO ₂	Al_2O_3	Fe ₂ O ₃	CaO	MgO
wt %	52.67	21.39	17.24	6.23	2.05

The ash was rich in silica and alumina, with iron oxide content exceeding 17 wt%, that makes it a suitable source for iron recovery [27,28].

Following concentrated sulfuric acid leaching (see Section 2.2 for details), the composition of the resulting solution is summarized in Table 2.

Table 2. Composition of the leachate obtained after leaching coal ash with concentrated sulfuric acid (g/L).

Component	Fe ²⁺	Fe³+	Fe (total)	Al ³⁺	Ca ²⁺	Mg ²⁺
g/L	18.4	3.3	21.7	6.8	0.9	1.7

As can be seen, Fe was efficiently leached, predominantly in the form of Fe²⁺, accompanied by minor Fe³⁺ and trace amounts of matrix elements such as Al³⁺, Ca²⁺, and Mg²⁺. The relatively low dissolution of Al can be attributed to its occurrence in refractory aluminosilicate phases such as mullite and glassy matrices, which are poorly reactive under acidic conditions. In addition, partial reprecipitation of Al³⁺ as amorphous Al(OH)₃ may occur during cooling or due to local pH gradients., accompanied by minor Fe³⁺ and trace amounts of matrix elements such as Al³⁺, Ca²⁺, and Mg²⁺.

The bulk pH of the solution remained within the range of 2.1-2.3, which is sufficiently low to suppress spontaneous precipitation of ferric hydroxides and enables stable electrochemical reduction of Fe²⁺. The moderate concentrations of aluminum and alkaline earth metals reduce the risk of co-deposition or passivation on the electrode surface, thus allowing selective iron recovery.

Thus, the physicochemical characteristics of the leachate (high Fe^{2+} content, low pH, and minimal interference from competing ions) indicate its suitability for downstream electrolytic iron deposition. This justifies further evaluation of key electrolysis parameters, such as current density, duration, and initial Fe^{2+} concentration, discussed in the following sections.

3.2. Electrolysis performance

Electrochemical Fe recovery from leach solutions is influenced by several key parameters, including Fe²⁺ concentration, current density, and electrolysis time. These factors control the rate of iron deposition, selectivity of the process, energy efficiency, and stability of the electrolyte. From a practical standpoint, they represent the main operational levers that can be adjusted during industrial implementation. To investigate their individual effects, a one-variable-at-a-time (OVAT) approach was used, where only one

parameter was varied while the others remained fixed [29]. The selected ranges were chosen based on hydrometallurgical practice, literature data, and preliminary experimental constraints. Fe2+ concentration was varied from 0.10 to 0.35 mol/L, covering the range from underleached to enriched solutions. Concentrations below 0.1 mol/L are known to result in low current efficiency due to mass transfer limitations, whereas concentrations above 0.35 mol/L may lead to increased viscosity, higher iron redissolution rates, and undesirable pH shifts. Current density was studied in the range of 1250 to 3750 A/m², which corresponds to practical levels used in metal electrowinning. Densities below 1000 A/m² often produce too slow a deposition rate, while those above 4000 A/m² tend to favor hydrogen evolution and reduce process selectivity. Electrolysis time was varied from 1 to 6 h in order to capture both the linear phase of deposition and possible saturation or redissolution effects at longer durations. The baseline Fe²⁺ concentration in the leachate was approximately 0.33 mol/L. To simulate deviations that may arise in real-world conditions - due to variations in ash composition, acid strength, or solid-to-liquid ratio - this value was either diluted or increased using FeSO₄·7H₂O to achieve the desired concentrations for electrolysis testing. Although a minor fraction of total Fe (~15%) was present as Fe3+, its influence on cathodic deposition was assumed to be negligible due to its relatively low concentration and slower reduction kinetics. In addition, the acidic environment and short electrolysis duration minimized the risk of Fe³⁺ hydrolysis and precipitation.

Table 3 shows the effect of the concentration of divalent iron on the current efficiency, iron recovery, and specific energy consumption per liter of solution; the density was maintained at 2500 A/m², and the electrolysis time was 4 h.

As shown in Table 3, increasing the initial Fe²⁺ concentration from 0.10 to 0.30 mol/L markedly improved both current efficiency and iron recovery. At the lowest concentration (0.10 mol/L), current efficiency was limited to 28%, and recovery reached only 45%, likely due to mass transport limitations and competitive hydrogen evolution. As the Fe²⁺level rose to 0.25-0.30 mol/L, current efficiency increased to 62-65%, and recovery improved to 85-89%, reflecting enhanced iron deposition at the cathode. A slight drop in efficiency at 0.35 mol/L (61%) may be associated with elevated ionic strength and side reactions, including partial redissolution of deposited iron. Notably, specific energy consumption

decreased with rising Fe²⁺ concentration, reaching a minimum of 1.8 Wh/L at 0.30 mol/L, indicating more efficient use of current for productive metal deposition. Based on these observations, 0.30 mol/L was selected as the optimal Fe²⁺ concentration for subsequent experiments, providing the highest efficiency and recovery at the lowest energy cost.

Table 3. Effect of Fe²⁺ concentration on current efficiency, iron recovery, and specific energy consumption (Wh/L) at a fixed current density of 2500 A/m² and electrolysis time of 4 h

[Fe²+], mol/L	Current efficiency, %	Fe recovery,%	Energy consumption, Wh/L
0.10	28	45	2.8
0.15	36	58	2.5
0.20	48	71	2.1
0.25	62	85	1.9
0.30	65	89	1.8
0.35	61	85	1.9

Figure 1 shows the effect of current density on the iron current efficiency and iron extraction into solid precipitate at $[Fe^{2+}] = 0.3 \text{ mol/L}$ and 4 h of electrolysis.

As illustrated in Fig. 1, the increase in current density from 1250 to 2500 A/m² led to a marked improvement in both current efficiency and iron recovery. The current efficiency rose from 34% to a maximum of 63%, while iron recovery increased from 53% to 87%. This behavior can be attributed to the enhanced cathodic kinetics and improved utilization of the applied current for Fe²+ reduction at moderate current densities. However, further

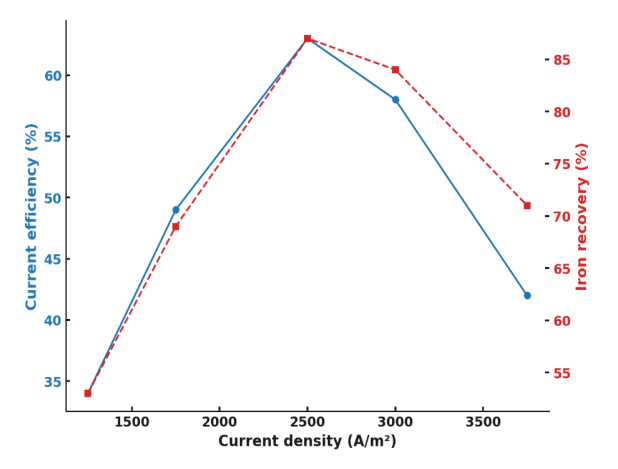


Fig. 1. Effect of current density on current efficiency and iron recovery at $[Fe^{2+}] = 0.30 \text{ mol/L}$ and electrolysis time of 4 h(T = 25 ± 2 °C).

increase to 3000 and 3750 A/m² resulted in a decline in both parameters. At the highest tested density (3750 A/m²), current efficiency dropped to 42% and iron recovery to 71%, likely due to intensified hydrogen evolution and possible redissolution of loosely bound iron deposits.

Figure 2 demonstrates the effect of current density on specific energy consumption; the content of divalent iron and electrolysis time were as in Fig. 1.

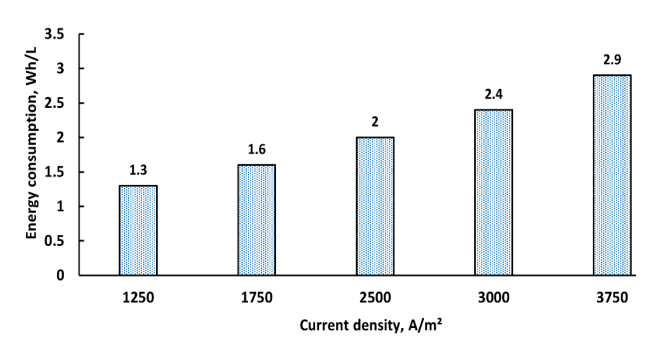


Fig. 2. Effect of current density on energy consumption at $[Fe^{2+}] = 0.30 \text{ mol/L}$ and electrolysis time of 4 h (T = 25 ± 2 °C).

As shown in Fig. 2, specific energy consumption increased steadily with current density. At the lowest tested density (1250 A/m²), energy consumption was minimal at 1.3 Wh/L. With increasing current density, the energy required per liter of electrolyte rose to 2.0 Wh/L at 2500 A/m² and reached 2.9 Wh/L at 3750 A/m². This trend reflects the greater electrical load applied to the system, as well as possible inefficiencies due to enhanced hydrogen evolution and reduced Faradaic efficiency at higher current inputs. Despite the high iron recovery at 2500 A/m², further increase in current density did not translate into proportional gains and led instead to unnecessary energy loss.

The current density of 2500 A/m² provided optimal process performance. At lower values (1250–1750 A/m²), the deposition rate was insufficient, and current was used inefficiently. Increasing the density to 3000-3750 A/m² led to higher energy consumption and reduced current efficiency. Thus, 2500 A/m² was chosen as the working value, ensuring a balance between metal yield and energy input.

Figure 3 shows the effect of electrolysis duration on the current efficiency and iron extraction into the cathode deposit at $[Fe^{2+}] = 0.3$ mol/L and current density of 2500 A/m².

Figure 3 shows that increasing electrolysis time from 1 to 4 h led to a gradual rise in iron recovery and current efficiency. Recovery improved from 36% to 89%, while current efficiency peaked at 65% after 3 h, then slightly declined to 63% at 4 h. Further

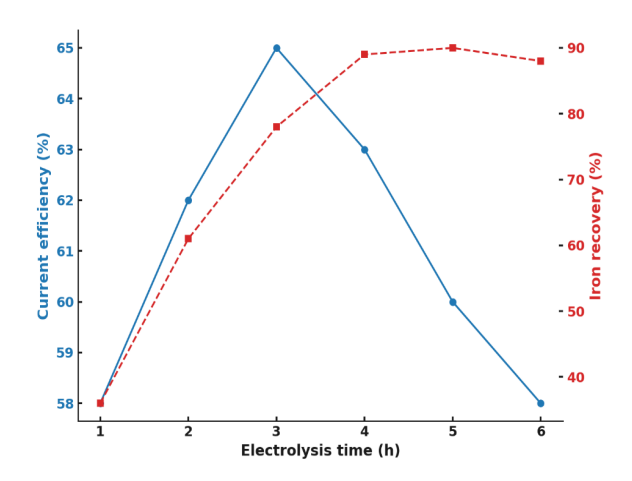


Fig. 3. Effect of electrolysis duration on current efficiency and iron recovery at [Fe2+] = 0.30 mol/L and current density of 2500 A/m² (T = 25 \pm 2 °C).

extension to 5 and 6 h resulted in marginal recovery gains (up to 90%) but a continuous drop in efficiency to 60% and 58%, respectively. The decrease is likely due to Fe2+ depletion and the onset of side reactions, including hydrogen evolution and partial redissolution of iron. A duration of 4 h was therefore considered sufficient to ensure high recovery with acceptable efficiency.

Monitoring pH during electrolysis is important for understanding reaction progression and ensuring solution stability. It reflects the balance between hydrogen ion consumption and generation, and helps prevent unwanted precipitation. Fig. 4 shows the change in pH over time under optimal electrolysis conditions.

As shown in Fig. 4, the pH of the electrolyte gradually increased from 2.2 to approximately 3.25 during the 6-h electrolysis process. This increase reflects the net consumption of hydrogen ions at the cathode, where two main reduction reactions take place [30]:

 $Fe^{2+} + 2e = Fe^{0}$

$$Fe^{2+} + 2e = Fe^{0}$$
(1)

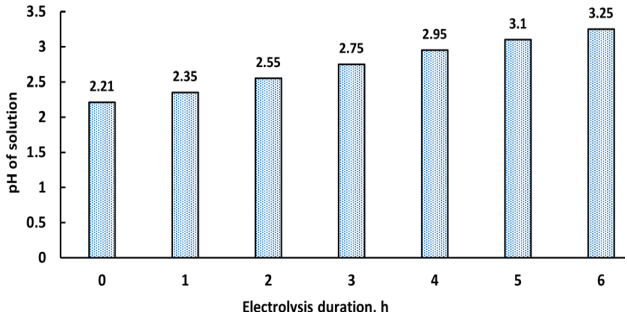


Fig. 4. Change in pH during electrolysis at [Fe²⁺] = 0.30 mol/L and current density of 2500 A/m² (T = 25 \pm 2 °C).

$$2H^+ + 2e = H_2$$
 (2)

These processes lower the proton concentration, thereby increasing the pH. Although anodic oxidation of water generates protons [31]:

$$2H_2O = O_2 + 4H^+ + 4e$$
 (3)

This is typically outweighed by the dominant cathodic consumption of H+, especially under galvanostatic conditions and with limited mixing.

A moderate rise in pH is generally beneficial for maintaining process stability; however, at elevated pH and prolonged operation, secondary reactions may occur. One such reaction is the partial oxidation of Fe2+ to Fe3+, followed by chemical or electrochemical formation of magnetite (Fe₃O₄):

$$Fe^{2+} + 2 Fe^{3+} + 8OH^{-} = Fe_3O_4 + H_2O$$
 (4)

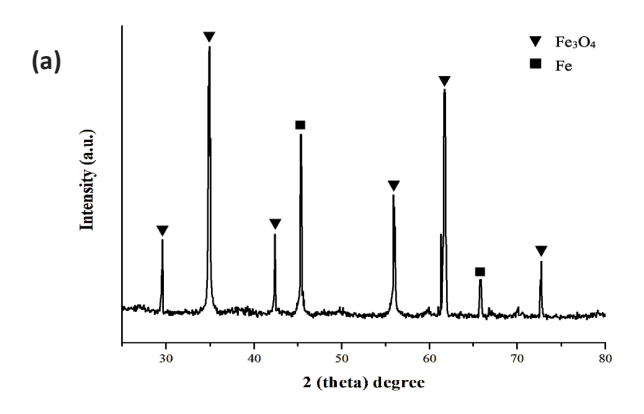
Alternatively, Fe₃O₄ may form electrochemically via:

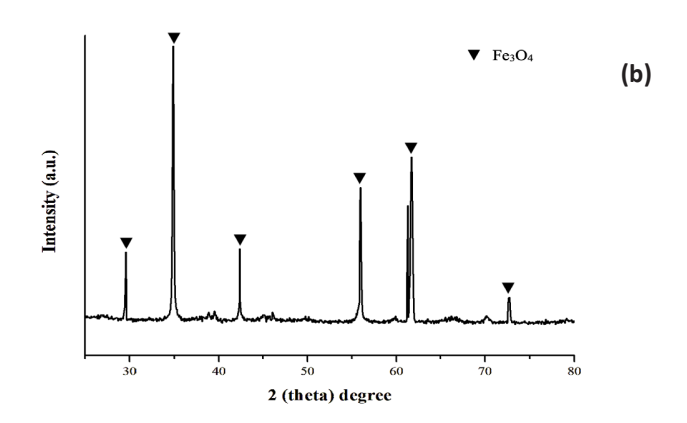
$$3Fe^{2+} + 4H_2O = Fe_3O_4 + 8H^+ + 2e$$
 (5)

The formation of Fe₃O₄ is favored under slightly acidic to near-neutral conditions and may account for black precipitates occasionally observed at intermediate stages.

Based on the obtained results, the optimal conditions for electrochemical iron recovery from coal ash leachate were established. A ferrous ion concentration of 0.30 mol/L ensured the highest current efficiency (65%) and Fe recovery (89%) while minimizing specific energy consumption (1.8 Wh/L). The best performance was achieved at a current density of 2500 A/m², which provided a favorable balance between deposition efficiency and energy input. An electrolysis duration of 4 h was found to be sufficient for near-complete recovery of Fe with minimal decline in current efficiency.

The results obtained in this study highlight the potential scalability of the proposed process. Electrochemical iron recovery can be adapted to continuous-flow electrowinning systems, which are already established in hydrometallurgical industries. Applying this approach to coal ash leachates provides a dual advantage: decreasing the volume of hazardous waste and generating metallic iron as a value-added product. Furthermore, integration of acid leaching and electrolysis into existing waste management or resource recovery schemes could facilitate its industrial implementation. However, further pilot-scale experiments are needed to assess electrode stability, energy efficiency under continuous operation, and process economics.





 $\textbf{Fig. 5.} \ XRD\ patterns\ of\ electrolysis\ products\ obtained\ under\ 0.20\ mol/L,\ 1750\ A/m^2,\ 4\ h\ (a)\ and\ 0.30\ mol/L,\ 2500\ A/m^2,\ 4\ h\ (b).$

3.3. Characterization of the electrolysis products

Fig. 5a shows the XRD pattern of the solid product obtained under mild electrolysis conditions ($[Fe^{2+}]$ = 0.20 mol/L, current density = 1750 A/m², electrolysis time = 4 h).

The diffractogram exhibits sharp peaks at $2\theta \approx 30.1^{\circ}$, 35.4° , 43.1° , 57.0° , 62.6° , and 74.7° which correspond to the characteristic reflections of magnetite (Fe₃O₄). The absence of metallic iron peaks suggests that under these conditions, the reduction of Fe²⁺ was incomplete, and the prevailing cathodic reactions, combined with local pH increase and possible oxidation of Fe²⁺ to Fe³⁺, led to precipitation of Fe₃O₄ via a mixed-valence route. This is consistent with known pathways of magnetite formation from Fe²⁺ and Fe³⁺ species under moderately acidic conditions.

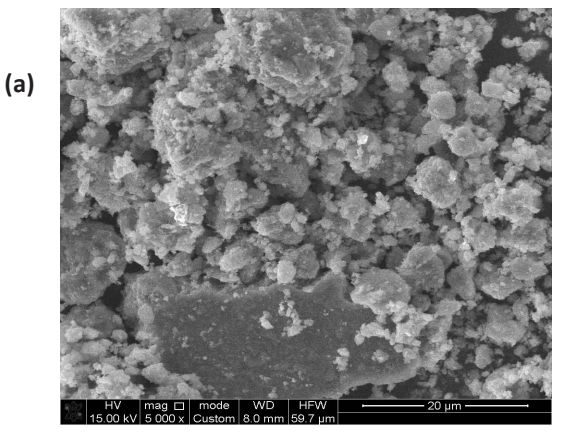
Fig. 5b, in contrast, shows the XRD pattern of the product obtained under optimized conditions ([Fe²⁺] = 0.30 mol/L, current density = 2500 A/m², time = 4 h). In this case, intense peaks appear at $2\theta \approx 44.7^{\circ}$ and 65.0°, corresponding to the metallic iron. Weaker reflections from Fe₃O₄ are still present, indicating that a small portion of the iron remained in oxide form, possibly due to partial air oxidation during handling

or concurrent electrochemical side reactions. The predominance of Fe in this sample confirms that higher Fe²⁺ concentration and adequate current density favor direct electrodeposition of metallic iron, as also supported by higher current efficiency and recovery metrics under these conditions.

Fig. 6a and 6b show SEM images of the solid products obtained under the same electrolysis conditions as in Fig. 5a and 5b, respectively.

The sample obtained under milder conditions (Fig. 6a) exhibits a porous structure composed of loosely aggregated spherical and submicron particles. This morphology is characteristic of Fe_3O_4 formed via indirect precipitation pathways involving Fe^{2+} and Fe^{3+} , consistent with the pure spinel phase observed in XRD.

By contrast, the product from the optimized electrolysis regime (Fig. 6b) reveals compact, flaky structures with irregular surfaces and embedded fine particles. This morphology reflects the presence of metallic Fe, formed via direct cathodic reduction, as confirmed by the additional Fe peaks in Fig. 5b. The mixed morphology suggests simultaneous deposition of Fe and Fe₃O₄, likely influenced by local concentration gradients and pH evolution during prolonged electrolysis.



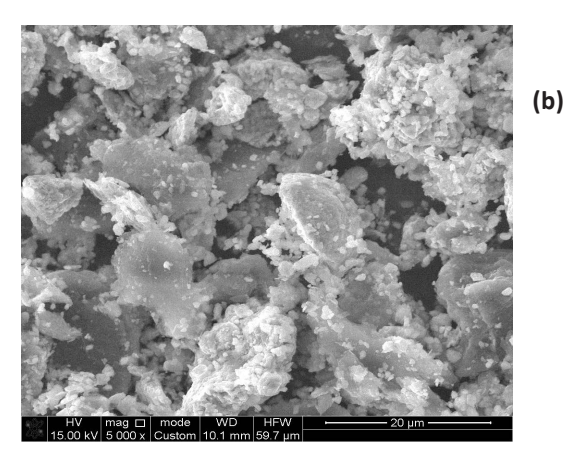


Fig. 6. SEM images of electrolysis products obtained under 0.20 mol/L, 1750 A/m², 4 h (a) and 0.30 mol/L, 2500 A/m², 4 h (b).

4. Conclusions

This study demonstrated the feasibility of electrochemical iron recovery from coal ash leachates obtained by concentrated sulfuric acid treatment. The leachate exhibited favorable characteristics, including high Fe2+ concentration (~0.30 mol/L) and low content of interfering ions, enabling selective electrodeposition. The effects of key parameters (Fe2+ concentration, current density, and electrolysis time) were investigated. Optimal performance was achieved at 0.30 $mol/L Fe^{2+}$, 2500 A/m², and 4 h, yielding 89% iron recovery and 65% current efficiency with minimal energy consumption (1.8 Wh/L). XRD and SEM characterization confirmed that mild conditions favored Fe₃O₄ formation via indirect pathways, whereas optimized parameters enabled direct Fe deposition with minor magnetite content.

The developed two-step process demonstrates practical potential for large-scale utilization of coal combustion residues by simultaneously reducing hazardous waste and generating metallic iron as a secondary resource. At the same time, certain limitations must be acknowledged, including the need for preliminary acid leaching, possible oxide by-product formation, and the requirement for pilot-scale validation. Our findings are also consistent with recent studies on leachingelectrowinning strategies for coal ash and related residues [7,17,18,22,23,26,31]. However, while those works mainly focused on leaching optimization or general electrowinning approaches, the present study provides a systematic evaluation of Fe²⁺ concentration, current density, and electrolysis duration for direct iron recovery from coal ash leachates. This distinction highlights both the novelty and the practical significance of our contribution within the most recent research landscape.

Funding

This work was funded by the Science Committee of the Ministry of Science and Higher Education of the Republic of Kazakhstan (Grant no. BR21882017).

References (GOST)

[1]. Kursun Unver I., Terzi M. Distribution of trace elements in coal and coal fly ash and their recovery with mineral processing practices: A review // J. Min. Environ. – 2018. – T. 9. – № 3. – C. 641–655.

- [2]. Shi W., Bai J., Kong L., Li H., Bai Z., Vassilev S. V., Li W. An overview of the coal ash transition process from solid to slag // Fuel. 2021. T. 287. C. 119537.
- [3]. Kong L., Bai J., Li W. Viscosity-temperature property of coal ash slag at the condition of entrained flow gasification: A review // Fuel Process. Technol. 2021. T. 215. C. 106751.
- [4]. Aleksandrova T., Nikolaeva N., Afanasova A., Chenlong D., Romashev A., Aburova V., Prokhorova E. Increase in recovery efficiency of iron-containing components from ash and slag material (coal combustion waste) by magnetic separation // Minerals. 2024. T. 14. № 2. C. 136
- [5]. Kamunur K., Batkal A., Mussapirova L., Ketegenov T. A. Separation of iron and carbon concentrates from thermal power plant solid waste using physical methods // Combust. Plasma Chem. 2024. T. 22. № 3. C. 223–230.
- [6]. Valeev D., Kunilova I., Alpatov A., Mikhailova A., Goldberg M., Kondratiev A. Complex utilisation of Ekibastuz brown coal fly ash: Iron & carbon separation and aluminum extraction // J. Clean. Prod. – 2019. – T. 218. – C. 192–201.
- [7]. Tian X., Guo Z., Zhu D., Pan J., Yang C., Li S. Recovery of valuable elements from coal fly ash: A review // Environ. Res. 2025. C. 121928.
- [8]. Rayzman V. L., Shcherban S. A., Dworkin R. S. Technology for chemical-metallurgical coal ash utilization // Energy Fuels. – 1997. – T. 11. – № 4. – C. 761–773.
- [9]. Seferinoğlu M., Paul M., Sandström Å., Köker A., Toprak S., Paul J. Acid leaching of coal and coalashes // Fuel. – 2003. – T. 82. – № 14. – C. 1721– 1734.
- [10]. Izquierdo M., Querol X. Leaching behaviour of elements from coal combustion fly ash: An overview // Int. J. Coal Geol. – 2012. – T. 94. – C. 54–66.
- [11]. Bhattacharya S. S., Kim K. H. Utilization of coal ash: Is vermitechnology a sustainable avenue? // Renew. Sustain. Energy Rev. 2016. T. 58. C. 1376—1386.
- [12]. Blissett R. S., Rowson N. A. A review of the multicomponent utilisation of coal fly ash // Fuel. – 2012. – T. 97. – C. 1–23.
- [13]. Revenko A. G., Pashkova G. V. Study of the chemical composition of coal and coal ash by X-ray fluorescence method: A review // X-Ray Spectrom. 2025. T. 54. № 2. C. 159–170.
- [14]. Paul M., Seferinoğlu M., Ayçık G. A., Sandström Å., Smith M. L., Paul J. Acid leaching of ash and coal:

- Time dependence and trace element occurrences // Int. J. Miner. Process. -2006. -T. 79. -N 1. -C. 27–41.
- [15]. Jones D. R. The leaching of major and trace elements from coal ash // Environ. Aspects Trace Elem. Coal. Dordrecht: Springer Netherlands, 1995. C. 221–262.
- [16]. Ketegenov T., Kamunur K., Mussapyrova L., Batkal A., Nadirov R. Enhancing rare earth element recovery from coal ash using high-voltage electrical pulses and citric acid leaching // Minerals. 2024. T. 14. № 7. C. 693.
- [17]. Mokoena K., Mokhahlane L. S., Clarke S. Effects of acid concentration on the recovery of rare earth elements from coal fly ash // Int. J. Coal Geol. 2022. T. 259. C. 104037
- [18]. Gao R., Peng H., He Q., Meng Z., Xiang P., Hou L., Miao Z. Simultaneous leaching of Li, Ga, and REEs from coal fly ash and a novel method for selective leaching of Li and Ga // J. Environ. Chem. Eng. 2024. T. 12. № 2. C. 112022.
- [19]. Wang P., Liu H., Zheng F., Liu Y., Kuang G., Deng R., Li H. Extraction of aluminum from coal fly ash using pressurized sulfuric acid leaching with emphasis on optimization and mechanism // JOM. 2021. T. 73. № 9. C. 2643–2651.
- [20]. Liu C. J., Zhao A. C., Ye X., Zhao Z., Yang X. R., Qin Y. M., Zhang T. A. Kinetics of aluminum extraction from roasting activated fly ash by sulfuric acid leaching // MRS Commun. 2024. T. 14. № 1. C. 48–55.
- [21]. Apua M. C., Nkazi B. D. Leaching of coal fly ash with sulphuric acid for synthesis of wastewater treatment composite coagulant // Can. Metall. Q. 2022. T. 61. № 3. C. 309–331.
- [22]. Valeev D., Shoppert A., Pankratov D., Cui J., Li F. Valorization of mullite-type coal fly ash via high-pressure NH₄HSO₄−H₂SO₄ leaching and selective iron (III) recovery by chelating resin // Sep. Purif. Technol. − 2025. − C. 134521.
- [23]. Lan S., Yang Y., Wang Z., Zheng Y., Li J., Zhao Q., Liu T. Study on membrane electrolysis for the removal of Fe from the leachate of coal fly ash // J. Environ. Chem. Eng. 2025. C. 117234.
- [24]. Cao W., Shu J., Chen J., Li Z., Zhou S., Liao S., Yang Y. Enhanced recovery of high-purity Fe powder from iron-rich electrolytic manganese residue by slurry electrolysis // Int. J. Miner. Metall. Mater. 2024. T. 31. № 3. C. 531–538.
- [25]. Duarte F., Lisenkov A. D., Kovalevsky A. V., Lopes D. V. Iron electrowinning from a nickel refinery residue for sustainable steelmaking // Electrochim. Acta. – 2025. – T. 515. – C. 145713.

- [26]. Liu Z., Guo X., Xu Z., Tian Q. Recent advancements in aqueous electrowinning for metal recovery: A comprehensive review // Miner. Eng. – 2024. – T. 216. – C. 108897.
- [27]. Cui L., Feng L., Yuan H., Cheng H., Cheng F. Efficient recovery of aluminum, lithium, iron and gallium from coal fly ash leachate via coextraction and stepwise stripping // Resour. Conserv. Recycl. 2024. T. 202. C. 107380.
- [28]. Wu M., Qi C., Chen Q., Liu H. Evaluating the metal recovery potential of coal fly ash based on sequential extraction and machine learning // Environ. Res. 2023. T. 224. C. 115546.
- [29]. Kavalsky L., Viswanathan V. Electrowinning for room-temperature ironmaking: Mapping the electrochemical aqueous iron interface // J. Phys. Chem. C. 2024. T. 128. № 35. C. 14611–14620.
- [30]. Zhang S., Yu J., Wang S., Liu Z., Wróblewski P. Electrodeposition behavior and characterization of Fe–P alloys at different pH values // Int. J. Electrochem. Sci. 2023. T. 18. № 11. C. 100323.
- [31]. Tan S. F., Wu H., Manser J. S., Zhang D., Ronchi M., Smullin S., Ross F. M. Electrochemical reactivity and stability of the Fe electrode in alkaline electrolyte // Adv. Funct. Mater. − 2025. − T. 35. − № 2. − C. 2407561.

References

- [1]. I. Kursun Unver, M. Terzi. Distribution of trace elements in coal and coal fly ash and their recovery with mineral processing practices: A review, J. Min. Environ. 9 (2018) 641–655. https://doi.org/10.22044/jme.2018.6855.1518.
- [2]. W. Shi, J. Bai, L. Kong, et al. An overview of the coal ash transition process from solid to slag, Fuel 287 (2021) 119537. https://doi.org/10.1016/j. fuel.2020.119537.
- [3]. L. Kong, J. Bai, W. Li. Viscosity—temperature property of coal ash slag at the condition of entrained flow gasification: A review, Fuel Process. Technol. 215 (2021) 106751. https://doi.org/10.1016/j.fuproc.2021.106751.
- [4]. T. Aleksandrova, N. Nikolaeva, et al. Increase in recovery efficiency of iron-containing components from ash and slag material (coal combustion waste) by magnetic separation, Minerals 14 (2024) 136. https://doi.org/10.3390/min14020136.
- [5]. K. Kamunur, A. Batkal, L. Mussapirova, et al. Separation of iron and carbon concentrates from thermal power plant solid waste using physical

- methods, Combust. Plasma Chem. 22 (2024) 223–230. https://doi.org/10.18321/cpc22(3)223-230.
- [6]. D. Valeev, I. Kunilova, A. Alpatov, et al. Complex utilisation of Ekibastuz brown coal fly ash: Iron & carbon separation and aluminum extraction, J. Clean. Prod. 218 (2019) 192–201. https://doi. org/10.1016/j.jclepro.2019.01.342.
- [7]. X. Tian, Z. Guo, D. Zhu, et al. Recovery of valuable elements from coal fly ash: A review, Environ. Res. 2025 121928. https://doi.org/10.1016/j. envres.2025.121928.
- [8]. V.L. Rayzman, S.A. Shcherban, R.S. Dworkin. Technology for chemical–metallurgical coal ash utilization, Energy Fuels 11 (1997) 761–773. https://doi.org/10.1021/ef960190s.
- [9]. M. Seferinoğlu, M. Paul, Å. Sandström, et al. Acid leaching of coal and coal ashes, Fuel 82 (2003) 1721–1734. https://doi.org/10.1016/S0016-2361(03)00132-7.
- [10]. M. Izquierdo, X. Querol. Leaching behaviour of elements from coal combustion fly ash: An overview, Int. J. Coal Geol. 94 (2012) 54–66. https://doi.org/10.1016/j.coal.2011.10.006.
- [11]. S.S. Bhattacharya, K.H. Kim. Utilization of coal ash: Is vermitechnology a sustainable avenue?, Renew. Sustain. Energy Rev. 58 (2016) 1376–1386. https://doi.org/10.1016/j.rser.2015.12.345.
- [12]. R.S. Blissett, N.A. Rowson. A review of the multi-component utilisation of coal fly ash, Fuel 97 (2012) 1–23. https://doi.org/10.1016/j. fuel.2012.03.024.
- [13]. A.G. Revenko, G.V. Pashkova. Study of the chemical composition of coal and coal ash by X-ray fluorescence method: A review, X-Ray Spectrom. 54 (2025) 159–170. https://doi.org/10.1002/ xrs.3444.
- [14]. M. Paul, M. Seferinoğlu, G. A. Ayçık, et al. Acid leaching of ash and coal: Time dependence and trace element occurrences, Int. J. Miner. Process. 79 (2006) 27–41. https://doi.org/10.1016/j. minpro.2005.11.008.
- [15]. D.R. Jones. The leaching of major and trace elements from coal ash, in: Environmental Aspects of Trace Elements in Coal, Springer Netherlands, Dordrecht, 1995, pp. 221–262. https://doi. org/10.1007/978-94-015-8496-8_12.
- [16]. T. Ketegenov, K. Kamunur, L. Mussapyrova, et al. Enhancing rare earth element recovery from coal ash using high-voltage electrical pulses and citric acid leaching, Minerals 14 (2024) 693. https://doi. org/10.3390/min14070693.
- [17]. K. Mokoena, L.S. Mokhahlane, S. Clarke. Effects of acid concentration on the recovery of rare

- earth elements from coal fly ash, Int. J. Coal Geol. 259 (2022) 104037. https://doi.org/10.1016/j. coal.2022.104037.
- [18]. R. Gao, H. Peng, Q. He, et al. Simultaneous leaching of Li, Ga, and REEs from coal fly ash and a novel method for selective leaching of Li and Ga, J. Environ. Chem. Eng. 12 (2024) 112022. https://doi.org/10.1016/j.jece.2024.112022.
- [19]. P. Wang, H. Liu, F. Zheng, et al. Extraction of aluminum from coal fly ash using pressurized sulfuric acid leaching with emphasis on optimization and mechanism, JOM 73 (2021) 2643–2651. https://doi.org/10.1007/s11837-021-04801-z.
- [20]. C.J. Liu, A.C. Zhao, X. Ye, et al. Kinetics of aluminum extraction from roasting activated fly ash by sulfuric acid leaching, MRS Commun. 14 (2024) 48–55. https://doi.org/10.1557/s43579-023-00494-4.
- [21]. M.C. Apua, B.D. Nkazi. Leaching of coal fly ash with sulphuric acid for synthesis of wastewater treatment composite coagulant, Can. Metall. Q. 61 (2022) 309–331. https://doi.org/10.1080/000 84433.2022.2044689.
- [22]. D. Valeev, A. Shoppert, D. Pankratov, et al. Valorization of mullite-type coal fly ash via highpressure NH₄HSO₄−H₂SO₄ leaching and selective iron(III) recovery by chelating resin, Sep. Purif. Technol. 2025, 134521. https://doi.org/10.1016/j. seppur.2025.134521.
- [23]. S. Lan, Y. Yang, Z. Wang, et al. Study on membrane electrolysis for the removal of Fe from the leachate of coal fly ash, J. Environ. Chem. Eng. 2025 117234. https://doi.org/10.1016/j.jece.2025.117234.
- [24]. W. Cao, J. Shu, J. Chen, et al. Enhanced recovery of high-purity Fe powder from iron-rich electrolytic manganese residue by slurry electrolysis, Int. J. Miner. Metall. Mater. 31 (2024) 531–538. https://doi.org/10.1007/s12613-023-2729-z.
- [25]. F. Duarte, A.D. Lisenkov, A.V. Kovalevsky, et al. Iron electrowinning from a nickel refinery residue for sustainable steelmaking, Electrochim. Acta 515 (2025) 145713. https://doi.org/10.1016/j. electacta.2025.145713.
- [26]. Z. Liu, X. Guo, Z. Xu, et al. Recent advancements in aqueous electrowinning for metal recovery: A comprehensive review, Miner. Eng. 216 (2024) 108897. https://doi.org/10.1016/j. mineng.2024.108897.
- [27]. L. Cui, L. Feng, H. Yuan, et al. Efficient recovery of aluminum, lithium, iron and gallium from coal fly ash leachate via coextraction and stepwise stripping, Resour. Conserv. Recycl.

- 202 (2024) 107380. https://doi.org/10.1016/j. resconrec.2023.107380.
- [28]. M. Wu, C. Qi, Q. Chen, et al. Evaluating the metal recovery potential of coal fly ash based on sequential extraction and machine learning, Environ. Res. 224 (2023) 115546. https://doi.org/10.1016/j.envres.2023.115546.
- [29]. L. Kavalsky, V. Viswanathan. Electrowinning for room-temperature ironmaking: Mapping the electrochemical aqueous iron interface, J. Phys. Chem. C 128 (2024) 14611–14620. https://doi. org/10.1021/acs.jpcc.4c01867.
- [30]. S. Zhang, J. Yu, S. Wang, et al. Electrodeposition behavior and characterization of Fe–P alloys at different pH values, Int. J. Electrochem. Sci. 18 (2023) 100323. https://doi.org/10.1016/j. ijoes.2023.100323.
- [31]. S. F. Tan, H. Wu, J. S. Manser, et al. Electrochemical reactivity and stability of the Fe electrode in alkaline electrolyte, Adv. Funct. Mater. 35 (2025) 2407561. https://doi.org/10.1002/adfm.202407561.

About the Authors

A. Batkal – PhD Student, Faculty of Chemistry and Chemical Technology, al-Farabi Kazakh National University, Almaty, Kazakhstan

E-mail: abatkalova@mail.ru ORCID: 0000-0002-2271-6953

K. Kamunur – PhD, Acting Associate Professor, Faculty of Chemistry and Chemical Technology, al-Farabi Kazakh National University, Almaty, Kazakhstan

E-mail: kamunur.k@mail.ru ORCID: 0000-0003-2160-9512

M.T. Yskak – Master student, Faculty of Chemistry and Chemical Technology, al-Farabi Kazakh National University, Almaty, Kazakhstan

E-mail: magzhanyskak02@mail.ru ORCID: 0009-0005-2700-0881

L.K. Beisembaeva – Associate Professor, Faculty of Chemistry and Chemical Technology, al-Farabi Kazakh National University, Almaty, Kazakhstan

E-mail: beisembaeva_l@mail.ru ORCID: 0000-0001-7529-673X

Электрохимическое извлечение железа из растворов сернокислого выщелачивания золошлака

А. Баткал*, К. Камунур, М.Т. Ыскак, Л.К. Бейсембаева

Казахский национальный университет им. аль-Фараби, пр. аль-Фараби, 71, Алматы, Казахстан

RNJATOHHA

Золошлак является одним из основных промышленных отходов и содержит значительные количества железа, однако его извлечение затруднено из-за инертной алюмосиликатной матрицы. В данной работе предложен двухстадийный подход для селективного извлечения и электрохимического восстановления железа. Золошлак подвергали обработке концентрированной серной кислотой при повышенной температуре, в результате чего получали раствор, обогащенный ионами Fe^{2+} . Электролиз проводили при различных условиях для оценки влияния концентрации Fe^{2+} , плотности тока и времени на степень извлечения железа, выход по току и удельный расход энергии. Оптимальные параметры (0,30 моль/л Fe^{2+} , 2500 A/ m^2 , 4 ч) обеспечили 89% извлечения железа при выходе по току 65% и низком энергопотреблении (1.8 $Br \cdot v / n$).

Ключевые слова: золошлак, сернокислотное выщелачивание, электроосаждение, электрохимическое извлечение железа, утилизация отходов.

Көмір күлінің күкірт қышқылды ерітінділерінен темірді электрохимиялық жолмен қалпына келтіру

А. Батқал*, Қ. Қамұнұр, М.Т. Ысқақ, Л.К. Бейсембаева

Әл-Фараби атындағы ҚазҰУ, әл-Фараби д., 71, Алматы, Қазақстан

АҢДАТПА

Көмір күлі — құрамында елеулі мөлшерде темір бар негізгі өнеркәсіптік қалдық, алайда инертті алюмосиликатты матрицаға байланысты оны қалпына келтіру күрделі мәселе болып қала береді. Осы зерттеуде темірді селективті түрде алу және электрохимиялық жолмен қалпына келтіру үшін екі сатылы әдіс әзірленді. Көмір күлі жоғары температурада концентрлі күкірт қышқылымен өңделіп, құрамында Fe^{2+} иондары мол еритін ерітінді алынды. Кейін электролиз әртүрлі жағдайларда жүргізіліп, Fe^{2+} концентрациясының, ток тығыздығының және электролиз уақытының темірді қалпына келтіру тиімділігіне, ток тиімділігіне және энергия шығынына әсері зерттелді. Оптималды жағдайларда (0,30 моль/л Fe^{2+} , 2500 A/м², 4 сағ) 89% темір қалпына келуі және 65% ток тиімділігі қамтамасыз етіліп, энергия шығыны 1,8 Вт·сағ/л деңгейіне дейін төмендеді.

Түйін сөздер: көмір күлі, күкірт қышқылымен шаймалау, электротұндыру, темірді электрохимиялық қалпына келтіру, қалдықтарды қайта пайдалану.